

A sparkless resistive glass correction electrode for the spherical proportional counter

I. Katsioulas,^{a,1} I. Giomataris,^a P. Knights,^{a,b} M. Gros,^a X.F. Navick,^a K. Nikolopoulos,^b I. Savvidis^c

^a*IRFU, CEA, Universite Paris-Saclay, F-91191 Gif-sur-Yvette, France*

^b*School of Physics and Astronomy, University of Birmingham, B15 2TT, United Kingdom*

^c*Aristotle University of Thessaloniki, Greece*

E-mail: ioannis.katsioulas@cea.fr

ABSTRACT: A new anode support structure for the spherical proportional counter is presented that incorporates a resistive correction electrode made of glass. This electrode improves the electric field homogeneity versus angle, while suppressing the probability and intensity of sparks compared to non-resistive alternatives. The configuration of the correction electrode was optimised with simulations. Such support structures have been constructed and measurements have demonstrated homogeneous response of the detector and operational stability. A measurement of the resistivity of the glass used is also presented.

KEYWORDS: Electronic detector readout concepts, Detector modelling and simulations II, Gaseous detectors, Materials for gaseous detectors, Dark Matter detectors, Very low-energy charged particle detectors

¹Corresponding author.

Contents

1	Introduction	1
2	Electric field configuration	3
3	The resistive correction electrode	4
3.1	Resistivity of the glass electrode	5
4	Development and performance of the resistive glass electrode prototypes	6
4.1	Voltage application on the glass electrode	7
4.2	Homogeneous response	7
4.3	Operational stability	9
5	Conclusions	9

1 Introduction

The Spherical Proportional Counter [1, 2] is a gaseous detector comprising a grounded spherical metallic shell acting as the cathode, and a small concentric sphere, the anode. The anode is supported by a grounded metallic rod. A wire through the centre of the rod supplies the anode high-voltage and the detector read-out. A review of recent developments in and applications of the spherical proportional counter is given in Ref. [3].

For the ideal case of a floating anode of radius r_1 at a voltage V_0 and located at the centre of a spherical cathode shell of radius r_2 , the magnitude of the radial electric field in the volume is

$$E(r) = \frac{V_0}{r^2} \frac{r_1 \cdot r_2}{r_2 - r_1}$$
$$\xrightarrow{r_1 \ll r_2} E(r) \approx \frac{V_0}{r^2} r_1 . \quad (1.1)$$

Equation 1.1 holds to a good approximation given that typically anode radii vary between 6 mm and 0.5 mm, with increasing gas pressure, while cathode radii are of $O(10 \text{ cm})$ or more. The r^{-2} dependence of the electric field naturally divides the detector into two regions: the drift and the multiplication volume. This is shown in Fig. 1, where electrons liberated in the drift volume will drift under the influence of the weak electric field towards the anode. Once a few millimetres from the anode, under the influence of the strong electric field, an avalanche will form. This dependence also leads to the drift time dispersion, $\sigma_t(r)$, of the initial electrons to be radius-dependent: $\sigma_t(r) \sim (r/r_2)^3$, a property exploited for detector fiducialisation. Furthermore, the difference in electron drift time between events with a spatially extended energy deposit versus those with a point-like energy deposit provides a powerful handle for background rejection [4–6]. Another feature of the detector is the very low capacitance, which is also practically independent

of the detector volume since for $r_1 \ll r_2$ it is given as $C \approx 4\pi\epsilon\epsilon_0 r_1$. This feature together with the large achievable gain [7] allows the development of large spherical proportional counters with an energy threshold as low as a single electron [8].

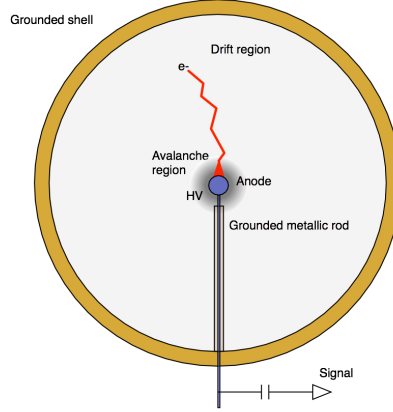


Figure 1. Schematic of a spherical proportional counter displaying the principle of operation.

These features suggest that the spherical proportional counter could be a good candidate for light dark matter searches, in the mass range from 0.1 GeV to 10 GeV [6], a possibility explored by the NEWS-G collaboration [9]. The detection relies on the measurement of low energy recoils, keV or lower, induced in the detector volume by elastic scattering of dark matter particles on the target nuclei. In this context, using detectors with sub-keV energy threshold gives a significant advantage, as discussed extensively in the literature [10–12]. The possibility to use various light targets, such as hydrogen, helium and neon, by changing the gas composition is also important, to maximize the recoil energy.

The NEWS-G Collaboration operates a 60 cm diameter detector in the Laboratoire Souterrain de Modane [13], which already yielded constraints on sub-GeV dark matter candidates [6]. A new spherical proportional counter with a gas volume of $O(m^3)$ is being developed, that will be operated under high pressure to further increase the target mass. The successful operation of the detector in high pressure and high gain relies heavily on the anode support structure, for response homogeneity, charge evacuation, and stability of operation. The inclusion of a correction electrode, which in the design described above is just the grounded rod, is essential: It shields the volume of the detector from the anode wire and improves the electric field homogeneity for zenith angles near the wire [2].

A second correction electrode could be placed a few millimetres from the anode surface, allowing the tuning of the electric field near the anode. However, having two electrodes with an electric potential difference between them in close proximity increases the probability of a discharge, making the detector unstable. This can be a limitation for the operation of the detector at high gain under high gas pressures. The addition of layers of insulators has been proposed and tested but with undesirable side-effects due to charging-up. In this article a different approach is presented, using electrodes made of a resistive material, specifically, lime-soda glass. Such materials have been used in other detectors to cover or act as electrodes [14, 15] and helped to improve detector operation.

2 Electric field configuration

The correction electrode plays an essential role for the electric field tuning in realistic detector geometries, affecting the uniformity of response of the detector as a function of the initial ionisation position. In its simplest form, the correction electrode is the grounded metallic rod, which shields the gas volume from the electric field of the anode wire. In the absence of the rod, a large fraction of the electric field lines would terminate on the wire, rather than the anode, resulting in the loss of ionisation electrons. The beneficial effect of the metallic rod is demonstrated by comparing the electric field configurations in Fig. 2(b) and 2(c), obtained with Finite Element Method (FEM) software [16], to the ideal case shown in Fig. 2(a). An extended analysis on the use of the metallic ground rod can be found in Ref. [2].

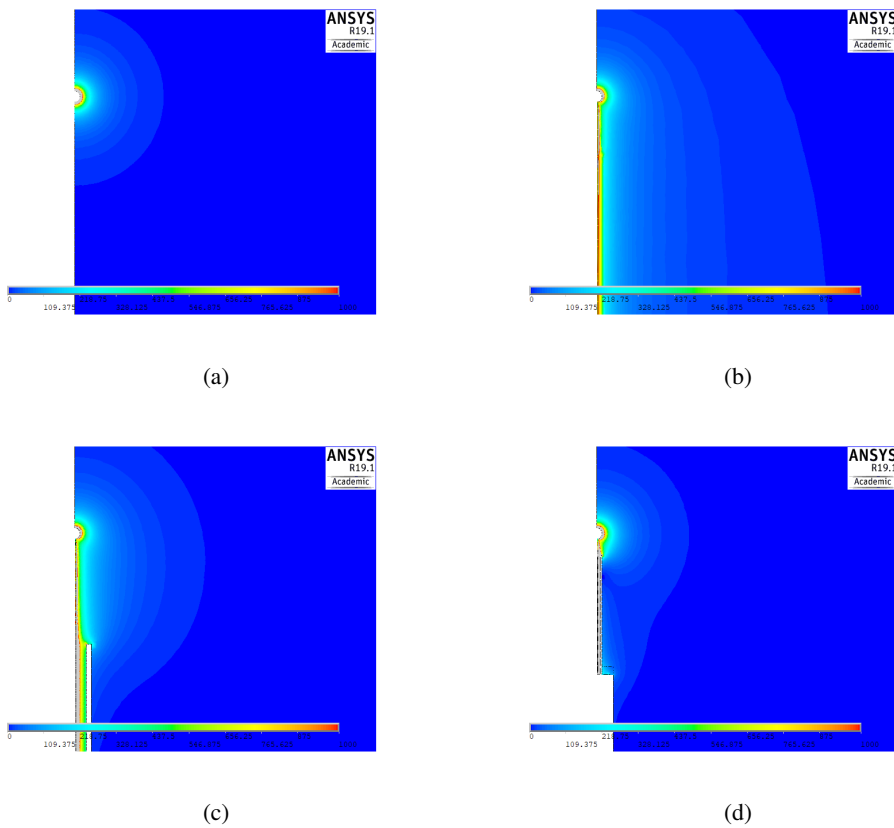


Figure 2. Electric field equipotential lines calculated using FEM software for a 15 cm radius spherical proportional counter with a 1 mm radius anode at 2000 V (a) for the ideal case comprising just the anode at high voltage, (b) including the anode wire to supply the high voltage, (c) including the grounded metallic rod surrounding the anode wire, and (d) including a second glass electrode placed 3 mm from the anode and set to 250 V.

Nevertheless, a more homogeneous electric field through the volume of the detector and close to the surface of the anode, can be obtained by adding a second correction electrode, complementary to the grounded metallic rod. This electrode is thinner, 1 mm to 2 mm in diameter, and shorter than the rod and it is placed a few millimeters from the anode surface. An independent electric voltage

can be applied to this electrode. The effect of the second correction electrode is shown in Fig. 2(d), providing higher electric field homogeneity and, thus, uniform response for large zenith angles, as demonstrated in Fig. 3(a). The electric field around the anode can be fine-tuned by varying the voltage on the surface of the second correction electrode. This is particularly important for the hemisphere containing the grounded rod, as shown in Fig. 3(b).

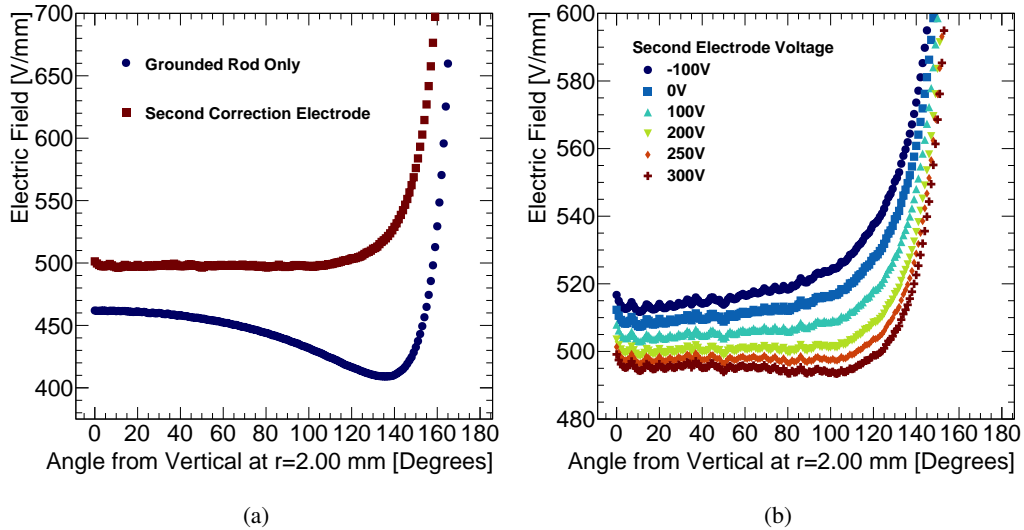


Figure 3. FEM calculation of the electric field as a function of the zenith angle calculated at a radius of 2 mm in an spherical proportional counter of radius 15 cm with a 1 mm radius anode set at 2000 V. (a) The comparison of the electric field for the case of a grounded rod surrounding the wire to the anode and the case where a second electrode is included. (b) The electric field for a second electrode consisting of 20 mm of glass located 3 mm from the anode for various applied voltages on the second correction electrode. A voltage of approximately 250 V provides the most homogeneous field for this geometry.

3 The resistive correction electrode

The correction electrode provides a simple but effective solution to the inhomogeneity of the electric field. However, to obtain the greatest control over the electric field it must be positioned only a few millimeters from the surface of the anode, supported by the grounded rod, which increases the probability of a discharge.

Following initial conceptual designs using FEM software, several prototypes were constructed. Testing of these prototypes has demonstrated that it is impractical to implement such a correction electrode using metallic or any conductive materials due to the increased sparking rate and intensity. A solution explored was the coating of the conductive material in an insulating layer, usually consisting of a layer of glue, Araldite®, or PLO plastic. However, the introduction of insulating materials close to the anode induces charging-up of the electrode and results in time-dependent gain variations, with time constants depending on geometry and operational conditions.

An alternative was found in the use of resistive materials as electrodes, which has been shown to reduce the spark rate and intensity in many detector designs, especially small gap micro-pattern

detectors [17–19]. Furthermore, using resistive materials for electrodes is an effective technique to achieve higher gain operation and increased operational stability. The resistivity in these materials, is high enough to quench sparks and allow normal detector operation in the occasion of a spark, while it is adequately low to prevent charging-up and, thus, time-dependent gain variations.

A series of resistive materials has been tested. Following the experience of resistive bulk Micromegas, initial tests involved polymer paste with resistivity in the $10^3 - 10^6 \Omega \cdot \text{cm}$ range. The construction of cylindrical electrodes at high precision when using paste was found to be challenging, while the obtained resistivity was inadequate for the desired effects.

Glass as a resistive material has been used to construct electrodes for various detectors including large surface Resistive Plate Chambers [14, 20, 21]. The glass electrode we used was in the form of a cylindrical tube with an 1.85(1.2) mm external (internal) diameter. The glass type was lime-soda glass [22], a common material used in a large number of applications.

3.1 Resistivity of the glass electrode

The volume resistivity, ρ , of the glass tube was measured based on a method described in Ref. [23]. The principle of measurement is presented in Fig. 4. The glass tube was sealed at one end with an insulating glue (Araldite) and heated at 200°C for a day to remove humidity from the surface. The tube was left to return to room temperature and was filled with an electrolyte of a salt water solution to a level L , shown in Fig. 4. It was then immersed up to this level in a container filled with the same electrolyte. By using two copper wires, one immersed into the container and one in the tube, the electric circuit is closed and a voltage is applied. Electrons must cross the volume of

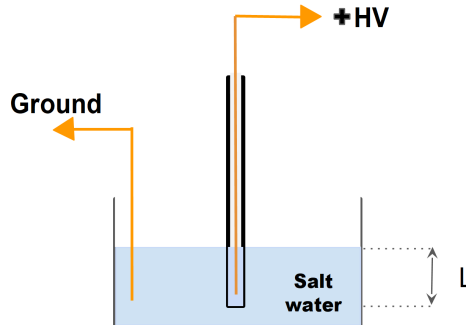


Figure 4. Resistivity measurement setup: The glass tube is filled with and immersed in the solution to depth L . A voltage is applied across the glass allowing measurement of the current through its volume.

glass to be collected by the electrode inside the tube and measured. The current I was measured as a function of the applied voltage V , up to 1 kV. A linear response is observed, as shown in Fig. 5. The resistivity of the glass tube is calculated from the average of measurements using,

$$\rho = \frac{2\pi LR}{\ln(b/a)}, \quad (3.1)$$

where $R = V/I$ is the resistance between the outer and inner surface of the tube, $L = 2.2$ cm, $a = 0.12$ cm ($b = 0.185$ cm) is the internal (external) diameter of the tube. The resistivity obtained

is $\rho = 5.05 \cdot 10^{10} \pm 27\% \Omega \cdot \text{cm}$. The uncertainty on the measured resistivity arises mainly from the limited accuracy of the electric current measurement in the voltage range between 0 V and 150 V.

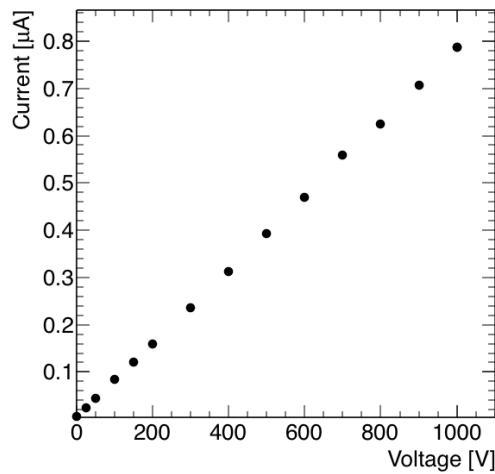


Figure 5. Current measured flowing through the glass versus applied voltage. From an average of these measurements, the resistivity of the glass tube was calculated as $\rho = 5.05 \cdot 10^{10} \pm 27\% \Omega \cdot \text{cm}$

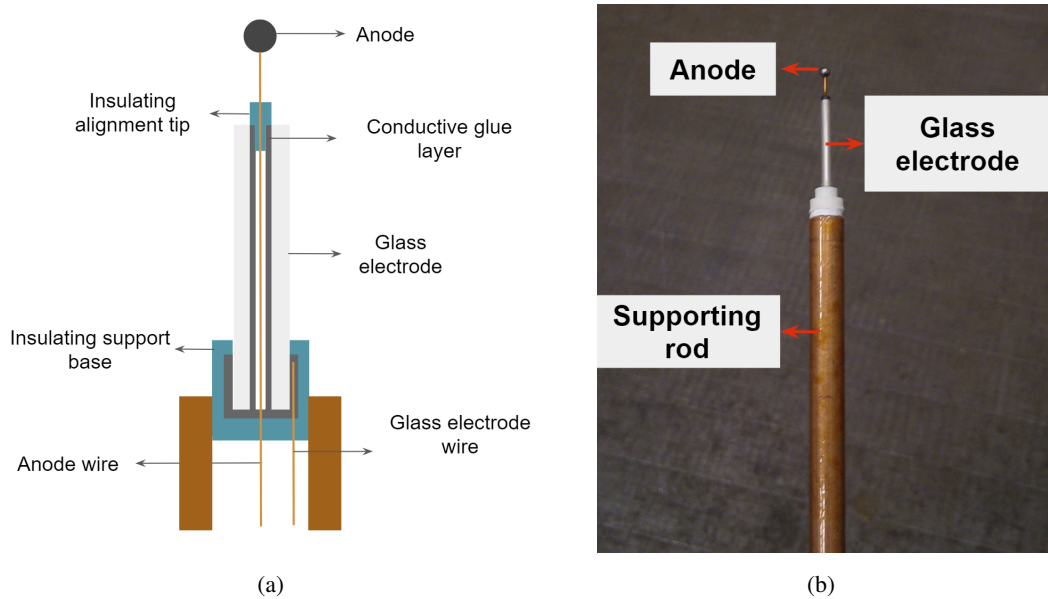


Figure 6. Module with a cylindrical glass correction electrode: (a) schematic and (b) implementation.

4 Development and performance of the resistive glass electrode prototypes

The rod with the glass electrode structure is presented in Fig. 6(a). The internal surface of the glass tube is covered with a layer of conductive glue and electric potential can be applied through a thin wire. This conductive layer facilitates the application of the electric potential on the glass

electrode and shields from the influence of the wire's electric field. The external part of the layer is covered with insulating glue, with a resistivity greater than $10^{14} \Omega \cdot \text{cm}$, to avoid sparks between the conductive layer and the rod. The wire of the anode passes through the glass tube and is aligned by a short insulating tip. The bottom part of the glass tube with the conductive layer and the insulating cover is placed in a insulating support base, made of PLO, constructed with high precision using 3D-printing. Finally, the support base is inserted into the rod.

In Fig. 6(b), the constructed module is presented.

The module is composed of a 2 mm diameter anode made of stainless steel. The anode is connected to the high voltage power supply with a thin wire, 150 μm in diameter, surrounded by a 200 μm thick insulating material. The glass tube has a length of 20 mm and the distance between the ending edge of the tube and the surface of the anode is 3 mm. The module is at the centre of a spherical, stainless steel vessel of 15 cm radius and is supported by a copper rod with a 4 mm (6 mm) inner (outer) diameter. The connection interface between the rod and the detector's spherical vessel ensures that both be grounded. The spherical vessel is 3 mm thick and is built to sustain pressure up to 10 bar. The module was tested for sparking in an argon atmosphere. The secondary electrode was grounded and the anode voltage gradually increased to 7000 V, without any sparks being observed.

In the following, tests of the performance of the 15 cm radius spherical proportional counter are presented. The counter was prepared by initially evacuating the spherical shell using a turbo-molecular pump, to a pressure of $5.37 \cdot 10^{-5} \text{ mbar} \cdot \text{L}$.

4.1 Voltage application on the glass electrode

A test was carried out to study the response of the module to a change in the voltage of the second correction electrode. The detector was filled with a gas of He:Ar:CH₄ (87%:10%:3%) at a pressure of 1 bar, with the anode voltage set to 1640 V. The high voltage applied on the glass electrode was varied to check that it is properly applied on the electrode surface. The voltage variations resulted in simultaneous gas gain variations. An example is displayed in Fig. 7 which shows the measured pulse amplitude as a function of time. Initially, the second correction electrode voltage was 100V, but was changed to 200 V after 8000 s, where the detector responded immediately with a gain drop.

4.2 Homogeneous response

To experimentally test the homogeneity of electric field achieved by the module, an ⁵⁵Fe source was placed inside the detector. The location of this collimated source could be changed during detector operation. ⁵⁵Fe decays through electron capture to ⁵⁵Mn emitting 5.9 keV X rays, on average. The detector was filled with 1 bar of He:Ar:CH₄ (92%:5%:3%) with the anode and second correction electrode voltages set at 1450 V and 200 V, respectively. Data were collected with the source located at 90° and 180° to the grounded rod and their amplitude distribution is shown in Fig. 8. At 180° any distortions to the electric field caused by the wire and grounded rod should be minimised. However, at 90° the X rays interact in a detector region potentially influenced by electric field distortions [3]. Such distortions could result in primary electrons arriving at the anode closer to the wire, leading to a worse energy resolution due to spatial gain variations. However, Fig. 8 demonstrate similar response in both cases. Thus, electric field distortions are corrected for by the second correction electrode.

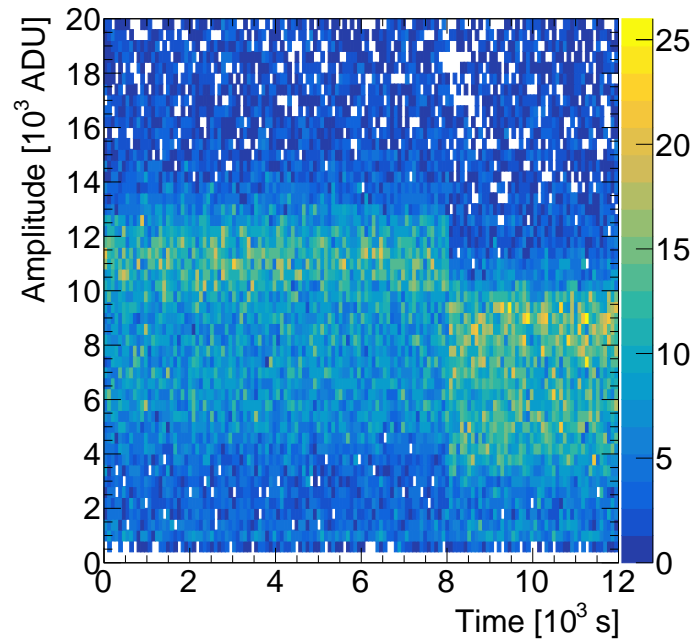


Figure 7. Amplitude versus time in a module with a second correction electrode. Initially, the second correction electrode voltage was at 100 V but was increased to 200 V at 8000 s.

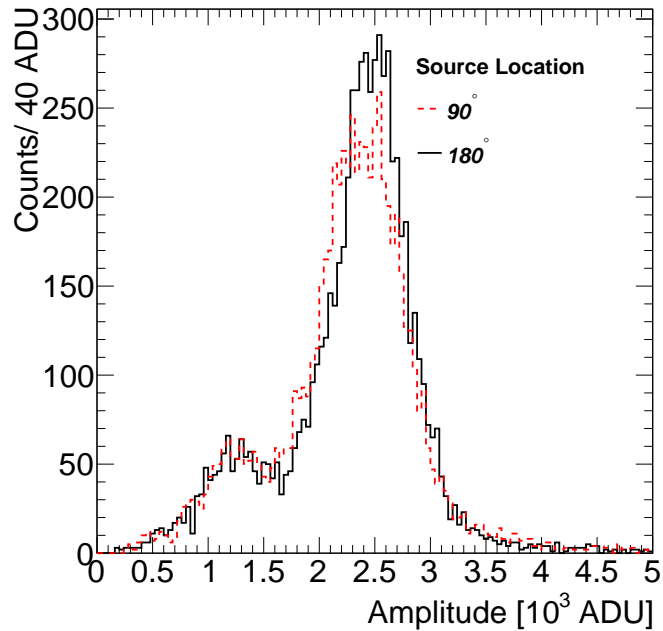


Figure 8. The overlaid amplitude distributions for the recorded pulses, for 5.9 keV X rays from an ^{55}Fe source located inside the detector placed at a zenith angle of 90° (red) and 180° (black), relative to the grounded rod.

4.3 Operational stability

The main goal was to be able to operate the detector in a gas pressure up to 2 bar and to avoid sparks when voltages over 2000 V were applied. To test the detector stability of operation, a gas of 2 bar of He:Ar:CH₄ (87%:10%:3%) was introduced into the detector through an Oxysorb® filter to remove oxygen and water traces from the gas. A voltage of 2350 V was applied to the anode with 0 V applied on the second correction electrode. To monitor the change in gain over time, the 6.4 keV X ray fluorescence of the ⁵⁵Fe K-line was used [8]. This fluorescence X ray is emitted homogeneously from the detector vessel stainless steel walls, induced mainly by environmental γ -rays and cosmic radiation. Data were collected for 12 days and the pulse height recorded versus time is shown in Fig. 9. A gradual decrease of the pulse height is observed which is caused by the introduction of contaminants due to the imperfect vacuum tightness of the detector. However, the detector was stable throughout the entire period, with no spark-induced gain variations.

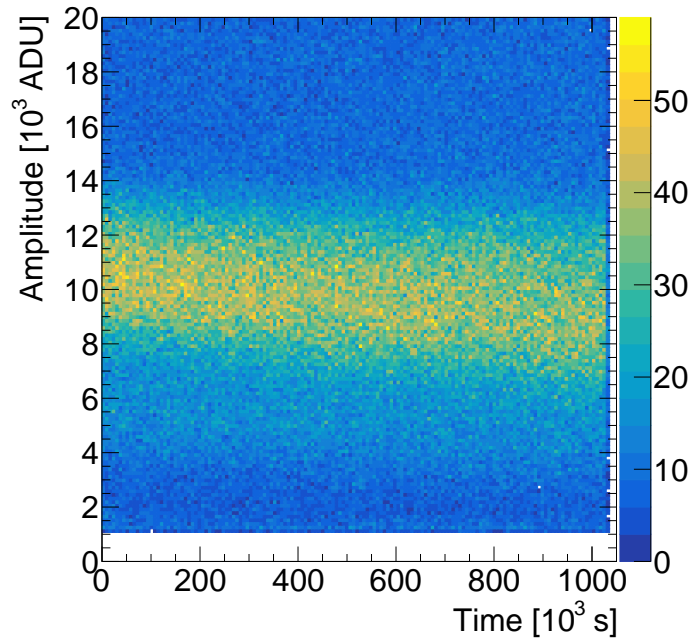


Figure 9. Pulse height as a function of time recorded using a module with a second correction electrode at 0 V, with an anode voltage of 2350 V in a detector filled with 2 bar of He:Ar:CH₄ (87%:10%:3%). The decrease in pulse height over time is due to contaminants, such as oxygen, leaking into the detector. Detector operation is stable and no discharges are observed.

5 Conclusions

Thanks to its versatility and features, the spherical proportional counter has found its way to a series of applications involving detection and measurement of low energy recoils, X rays, α -particles, protons, γ -rays, and neutrons. Most of these applications require the detector to operate in high pressure with a relatively high gain, and long-term stability. Also good energy resolution and homogeneous response is important for these applications. The use of a correction electrode, on

which a second voltage can be applied, is an effective solution to achieve these goals. The proposed design featuring a glass resistive electrode provides a handle to fine-tune the electric field near the anode, optimise the resolution for given operation conditions, while suppressing sparks and ensuring long time operation stability.

Acknowledgments

This work was performed within the NEWS-G collaboration and has received funding by the French National Research Agency (ANR-15-CE31-0008).

References

- [1] I. Giomataris, et al., NOSTOS experiment and new trends in rare event detection, Nucl. Phys. Proc. Suppl. 150 (2006) 208–213, [,208(2005)]. [arXiv:hep-ex/0502033](https://arxiv.org/abs/hep-ex/0502033), [doi:10.1016/j.nuclphysbps.2005.01.245](https://doi.org/10.1016/j.nuclphysbps.2005.01.245).
- [2] I. Giomataris, I. Irastorza, I. Savvidis, S. Andriamonje, S. Aune, M. Chapellier, P. Charvin, P. Colas, J. Derre, E. Ferrer, M. Gros, X. F. Navick, P. Salin, J. D. Vergados, A novel large-volume spherical detector with proportional amplification read-out, J. Instrum. 3 (09) (2008) P09007.
- [3] Q. Arnaud, A. Brossard, A. Dastgheibi-Fard, G. Gerbier, I. Giomataris, I. Katsioulas, P. Knights, K. Nikolopoulos, I. Savvidis, Savvidis, Spherical Proportional Counter: A review of recent developments, J. Phys. Conf. Ser. 1029 (1) (2018) 012006. [doi:10.1088/1742-6596/1029/1/012006](https://doi.org/10.1088/1742-6596/1029/1/012006).
- [4] E. Bougamont, A. Dastgheibi, J. Derre, J. Galan, G. Gerbier, I. Giomataris, M. Gros, I. Katsioulas, D. Jourde, P. Magnier, X. F. Navick, T. Papaevangelou, I. Savvidis, G. Tsiledakis, Neutron spectroscopy with the spherical proportional counter based on nitrogen gas, Nucl. Instrum. Methods Phys. Res. A 847 (2017) 10–14.
- [5] I. Savvidis, I. Katsioulas, C. Eleftheriadis, I. Giomataris, T. Papaevangelou, Low energy recoil detection with a spherical proportional counter, Nucl. Instrum. Methods Phys. Res. A 877 (2018) 220–226.
- [6] NEWS-G Collaboration, Q. Arnaud, D. Asner, J.-P. Bard, A. Brossard, B. Cai, M. Chapellier, M. Clark, E. C. Corcoran, T. Dandl, A. Dastgheibi-Fard, K. Dering, P. Di Stefano, D. Durnford, G. Gerbier, I. Giomataris, P. Gorel, M. Gros, O. Guillaudin, E. W. Hoppe, A. Kamaha, I. Katsioulas, D. G. Kelly, R. D. Martin, J. McDonald, J.-F. Muraz, J.-P. Mols, X.-F. Navick, T. Papaevangelou, F. Piquemal, S. Roth, D. Santos, I. Savvidis, A. Ulrich, F. Vazquez de Sola Fernandez, M. Zampaolo, First results from the NEWS-G direct dark matter search experiment at the LSM, Astropart. Phys. 97 (2018) 54–62.
- [7] F. J. Iguaz Gutierrez, A. Rodriguez, J. F. Castel, I. G. Irastorza, Characterization of a spherical proportional counter in argon-based mixtures, in: Proceedings of Technology and Instrumentation in Particle Physics 2014 — PoS(TIPP2014), Sissa Medialab, Trieste, Italy, 2015, p. 162.
- [8] E. Bougamont, P. Colas, J. Derre, I. Giomataris, G. Gerbier, M. Gros, P. Magnier, X. F. Navick, P. Salin, I. Savvidis, G. Tsiledakis, J. D. Vergados, Ultra low energy results and their impact to dark matter and low energy neutrino physics [arXiv:1010.4132](https://arxiv.org/abs/1010.4132).
- [9] NEWS-G, <https://news-g.org>.

- [10] R. Agnese, A. J. Anderson, M. Asai, D. Balakishiyeva, R. Basu Thakur, D. A. Bauer, J. Beaty, J. Billard, A. Borgland, M. A. Bowles, D. Brandt, P. L. Brink, R. Bunker, B. Cabrera, D. O. Caldwell, D. G. Cerdeno, H. Chagani, Y. Chen, M. Cherry, J. Cooley, B. Cornell, C. H. Crewdson, P. Cushman, M. Daal, D. DeVaney, P. C. F. Di Stefano, E. D. C. E. Silva, T. Doughty, L. Esteban, S. Fallows, E. Figueroa-Feliciano, G. L. Godfrey, S. R. Golwala, J. Hall, S. Hansen, H. R. Harris, S. A. Hertel, B. A. Hines, T. Hofer, D. Holmgren, L. Hsu, M. E. Huber, A. Jastram, O. Kamaev, B. Kara, M. H. Kelsey, S. Kenany, A. Kennedy, M. Kiveni, K. Koch, A. Leder, B. Loer, E. Lopez Asamar, R. Mahapatra, V. Mandic, C. Martinez, K. A. McCarthy, N. Mirabolfathi, R. A. Moffatt, R. H. Nelson, L. Novak, K. Page, R. Partridge, M. Pepin, A. Phipps, M. Platt, K. Prasad, M. Pyle, H. Qiu, W. Rau, P. Redl, A. Reisetter, R. W. Resch, Y. Ricci, M. Ruschman, T. Saab, B. Sadoulet, J. Sander, R. L. Schmitt, K. Schneck, R. W. Schnee, S. Scorza, D. N. Seitz, B. Serfass, B. Shank, D. Speller, A. Tomada, S. Upadhyayula, A. N. Villano, B. Welliver, D. H. Wright, S. Yellin, J. J. Yen, B. A. Young, J. Zhang, (SuperCDMS Collaboration), Search for low-mass weakly interacting massive particles with SuperCDMS, *Phys. Rev. Lett.* 112 (24) (2014) 241302.
- [11] DAMIC Collaboration, A. Aguilar-Arevalo, D. Amidei, X. Bertou, M. Butner, G. Canelo, A. Castañeda Vázquez, B. A. Cervantes Vergara, A. E. Chavarria, C. R. Chavez, J. R. T. de Mello Neto, J. C. D’Olivo, J. Estrada, G. Fernandez Moroni, R. Gaior, Y. Guardincerri, K. P. Hernández Torres, F. Izraelevitch, A. Kavner, B. Kilminster, I. Lawson, A. Letessier-Selvon, J. Liao, V. B. B. Mello, J. Molina, J. R. Peña, P. Privitera, K. Ramanathan, Y. Sarkis, T. Schwarz, C. Sengul, M. Settimo, M. Sofo Haro, R. Thomas, J. Tiffenberg, E. Tiouchichine, D. Torres Machado, F. Trillaud, X. You, J. Zhou, Search for low-mass WIMPs in a 0.6 kg day exposure of the DAMIC experiment at SNOLAB, *Phys. Rev. D* 94 (8) (2016) 082006.
- [12] The CRESST Collaboration, G. Angloher, A. Bento, C. Bucci, L. Canonica, A. Erb, F. v. Feilitzsch, N. Ferreira Iachellini, P. Gorla, A. Gütlein, D. Hauff, J. Jochum, M. Kiefer, H. Kluck, H. Kraus, J. C. Lanfranchi, J. Loebell, A. Münster, F. Petricca, W. Potzel, F. Pröbst, F. Reindl, K. Schäffner, J. Schieck, S. Scholl, S. Schönert, W. Seidel, L. Stodolsky, C. Strandhagen, R. Strauss, A. Tanzke, M. Uffinger, A. Ulrich, I. Usherov, S. Wawoczny, M. Willers, M. Wüstrich, A. Zöller, Probing low WIMP masses with the next generation of CRESST detector [arXiv:1503.08065](https://arxiv.org/abs/1503.08065).
- [13] "Laboratoire Souterrain de Modane (LSM)", <http://www-lsm.in2p3.fr/>.
- [14] M. Naimuddin, D. Kaur, P. Kumar, A. Gaur, M. Hasbuddin, S. Mishra, A. Kumar, Characterisation of glass electrodes and rpc detectors for INO-ICAL experiment, *J. Instrum.* 9 (10) (2014) C10039.
- [15] R. Kanishka, V. Bhatnagar, D. Indumathi, Optimisation and characterisation of glass RPC for india-based neutrino observatory detectors [arXiv:1605.09361](https://arxiv.org/abs/1605.09361).
- [16] S. S. Rao, Chapter 22 - finite element analysis using ANSYS FEM software is marketed by ANSYS, inc., southpointe, 275 technology drive, canonsburg, PA 15317, in: S. S. Rao (Ed.), *The Finite Element Method in Engineering (Sixth Edition)*, Butterworth-Heinemann, 2018, pp. 703–721.
- [17] T. Alexopoulos, J. Burnens, R. de Oliveira, G. Glonti, O. Pizzirusso, V. Polychronakos, G. Sekhniaidze, G. Tsigopolitis, J. Wotschack, A spark-resistant bulk-micromegas chamber for high-rate applications, *Nucl. Instrum. Methods Phys. Res. A* 640 (1) (2011) 110–118.
- [18] J. Wotschack, Development of micromegas muon chambers for the ATLAS upgrade, *J. Instrum.* 7 (02) (2012) C02021.
- [19] A. Yoshikawa, T. Tamagawa, T. Iwahashi, F. Asami, Y. Takeuchi, A. Hayato, H. Hamagaki, T. Gunji, R. Akimoto, A. Nukariya, S. Hayashi, K. Ueno, A. Ochi, R. Oliveira, Development of resistive electrode gas electron multiplier (RE-GEM), *J. Instrum.* 7 (06) (2012) C06006.

- [20] W. Riegler, C. Lippmann, The physics of resistive plate chambers, Nucl. Instrum. Methods Phys. Res. A 518 (1) (2004) 86–90.
- [21] V. M. Datar, S. Jena, S. D. Kalmani, N. K. Mondal, P. Nagaraj, L. V. Reddy, M. Saraf, B. Satyanarayana, R. R. Shinde, P. Verma, Development of glass resistive plate chambers for INO experiment, Nucl. Instrum. Methods Phys. Res. A 602 (3) (2009) 744–748.
- [22] Soda-lime glass, <https://www.britannica.com/technology/soda-lime-glass>.
- [23] J. A. Coles, J. L. Munoz, F. Deyhimi, Surface and volume resistivity of pyrex glass used for liquid membrane Ion-Sensitive microelectrodes, in: M. Kessler, D. K. Harrison, J. Höper, R. P. Buck, G. Eisenman, J. Hill, R. N. Khuri, D. W. Lübbers, C. Nicholson, W. Simon, T. Treasure, T. Zeuthen (Eds.), Ion Measurements in Physiology and Medicine, Springer Berlin Heidelberg, Berlin, Heidelberg, 1985, pp. 67–73.